Supporting Information

Recovering Mechanoluminescence in SAOED/Epoxy Stress Sensors with Self-Healing Epoxy Vitrimers

Cigdem Caglayan [a], Geonwoo Kim [a], Gun Jin Yun [a, b,1]

[a] Department of Aerospace Engineering, Seoul National University, Seoul, South Korea, 08826

[b] Institute of Advanced Aerospace Engineering Technology, Seoul National University, Seoul, Korea, 08826

1. Synthesis of siloxane bond-exchange hardener (K-PAMS)

Based on previously reported literature studies 1-3, the siloxane bond-exchange hardener is synthesized in the laboratory. Oligo-aminopropyl-methyl-diethoxy-silane (PAMS) is synthesized by reacting 2 moles of distilled water with 1 mol of APEMS at 90°C for six hours under reflux. The water and generated ethanol are removed by vacuum distillation to obtain the product, PAMS. The potassium silanolate derivative of PAMS (K-PAMS) is synthesized by adding PAMS and five wt% KOH into a round bottom flask equipped with a distilling condenser. The mixture is stirred at 110°C for four hours until no more water is produced. During the process, byproducts are collected by distilling condenser, yielding to a viscous liquid.

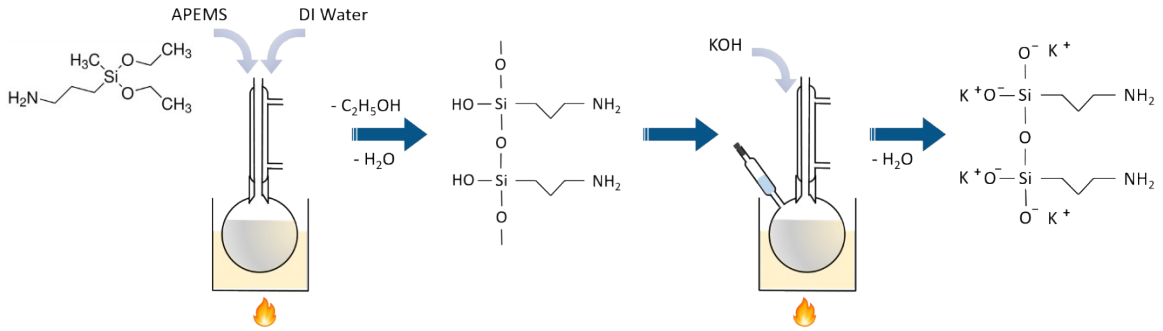

Figure S1: Synthesis route of K-PAMS to be used in the fabrication of siloxane bond-exchange based ML stress sensors

2. Characterization of K-PAMS

[1] Corresponding author: Professor, Department of Aerospace Engineering, Seoul National University, Gwanak-gu, Gwanak-ro 1, New Engineering Building 301, Room 1308, Tel:+82-2-880-8302, Email: gunjin.yun@snu.ac.kr

The characterization of K-PAMS by FTIR and H-NMR demonstrates the successful synthesis of polysiloxane oligomer with catalytic potassium silanolate end groups. According to FTIR, the 1000-1100 cm^{-1} spectral region corresponding to Si-O-Si bonds becomes a single strong peak within the hydrolysis of APEMS. In H-NMR, new peaks appear at (0.37 ppm, 2H: Si-CH_2), (0.27 ppm, 2H: Si-CH_2), (-0.10 ppm, 3H: Si-CH_3), (-0.20 ppm, 3H: Si-CH_3) indicate more Si-O units are terminated with Si-O-K^+ groups with the introduction of KOH [1].

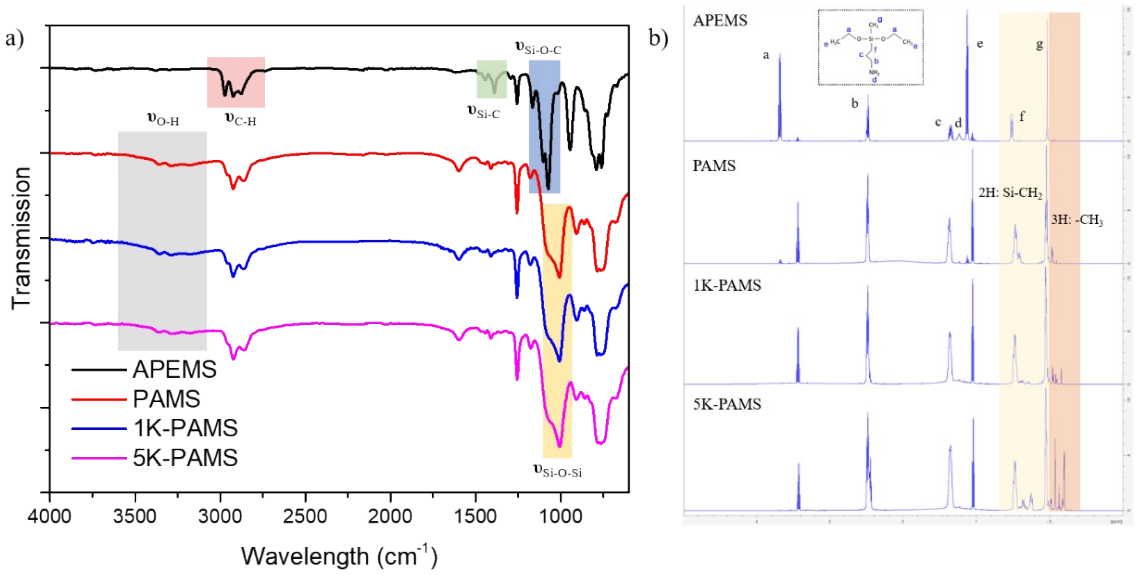

Figure S2: a) FTIR and b)H-NMR spectra of synthesized K-PAMS hardener

3. Thermal and mechanical performance of ML stress sensors

The mechanical properties of ML stress sensors are evaluated through tension tests. Table S1 highlights the importance of controlling the SAOED concentration to achieve optimal mechanical performance.

Table S1: Varying stiffness and ultimate tensile strength of ML stress sensors

Sample	Young's Modulus (GPa)	Ultimate Tensile Strength (MPa)
Ep	1.4 ± 0.01	77.5 ± 1.9
10-ML/Ep	1.4 ± 0.05	64.5 ± 1.9
20-ML/Ep	1.4 ± 0.05	44.0 ± 1.6
VT	1.5 ± 0.02	90.2 ± 3.5
10-ML/VT	1.5 ± 0.03	60.6 ± 1.3
20-ML/VT	1.5 ± 0.09	47.3 ± 0.9
SVT	0.9 ± 0.03	57.9 ± 0.8
10-ML/SVT	1.0 ± 0.07	53.5 ± 0.7
20-ML/SVT	1.0 ± 0.05	39.4 ± 0.3

In addition, thermal stability of ML stress sensors are investigated using TGA. The decomposition temperatures at 5% and 50% exhibits opposite trends in the cases of 20-ML/Ep and 20-ML/SVT, Table S2.

Table S2: Thermal stability of ML stress sensors tested under nitrogen atmosphere

Sample	Thermal stability	
	$T_d^{5\%}$ (°C)	$T_d^{50\%}$ (°C)
20-ML/Ep	328.9	391.5
20-ML/VT	277.7	369.5
20-ML/SVT	204.4	480.6

Figure S3 displays the morphology of 20-ML/SVT surface trimmed using a microtome diamond blade. SAOED particles are observed to distribute uniformly within the polymer matrix, taking particle size and shape variation into account.

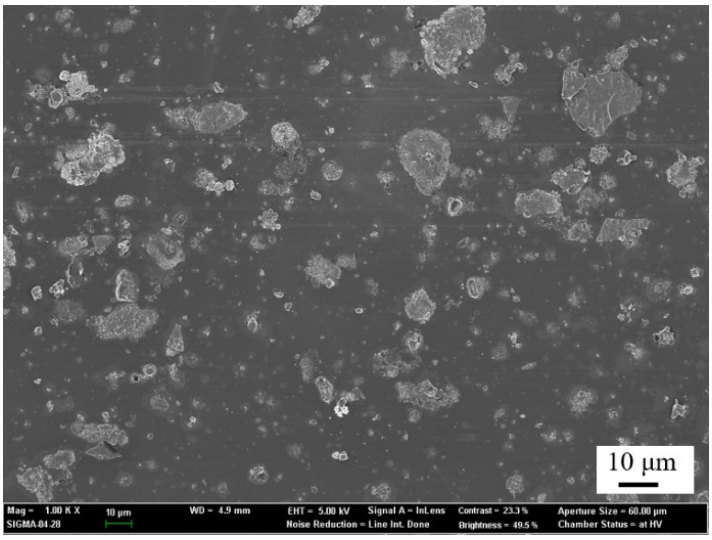

Figure S3: SEM image of 20-ML/SVT demonstrating the quality of dispersion and distribution

4. Optical properties of ML stress sensors

Photoluminescence spectra is acquired using a FluoTime 300 spectrometer (PicoQuant), while light transmittance measurements are conducted with a V-770 spectrophotometer (Jasco) at room temperature.

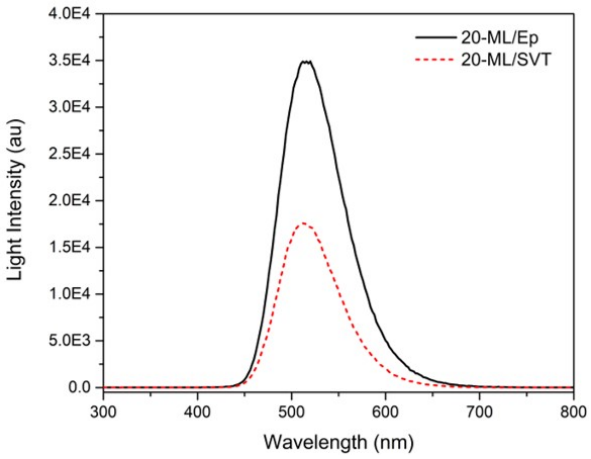

Figure S4: Steady-state photoluminescence spectrum of ML stress sensors excited by Xe lamp (290nm)

The photoluminescence of 20-ML/Ep is observed to be higher than that of 20-ML/SVT, Figure S4, with a maximum light emission approximately at 510nm. Table S3 highlights the light transmittance of ML stress sensors in the visible spectrum. The transmittance of both samples are mostly identical, except 20-ML/Ep having a relatively lower transmittance than 20-ML/SVT at 510nm. These findings suggest that commercial epoxy exhibits a higher absorbtion of the emitted light, potentially due to higher reflection

and scattering within its densely packed structure. This would also contribute to greater light extraction and a higher PL intensity. In contrast, the higher transmittance and lower PL intensity in siloxane-bond exchange based epoxy are attributed to the faster escape of emitted light rather than internal reflection or scattering given its less crosslinked and relatively less restricted structure.

Table S3: Transmittance of ML stress sensors with a thickness of 3±0.2mm

Sample	Transmission (%) at wavelengths		
	400nm	510nm emission max	600nm
20-ML/Ep	1.8%	19.3%	24.9%
20-ML/SVT	1.6%	24.4%	25.9%

5. Void fraction estimation in ML stress sensors by XRM analysis

The morphological characterization of ML stress sensors before and after cyclic tensile testing is performed using XRM analysis. The samples are scanned at a high magnification of 2*x*2 pixels, and the images are analyzed using MATLAB®. Void formation around SAOED particles is evaluated approximately by following the given algorithm in Figure S5.

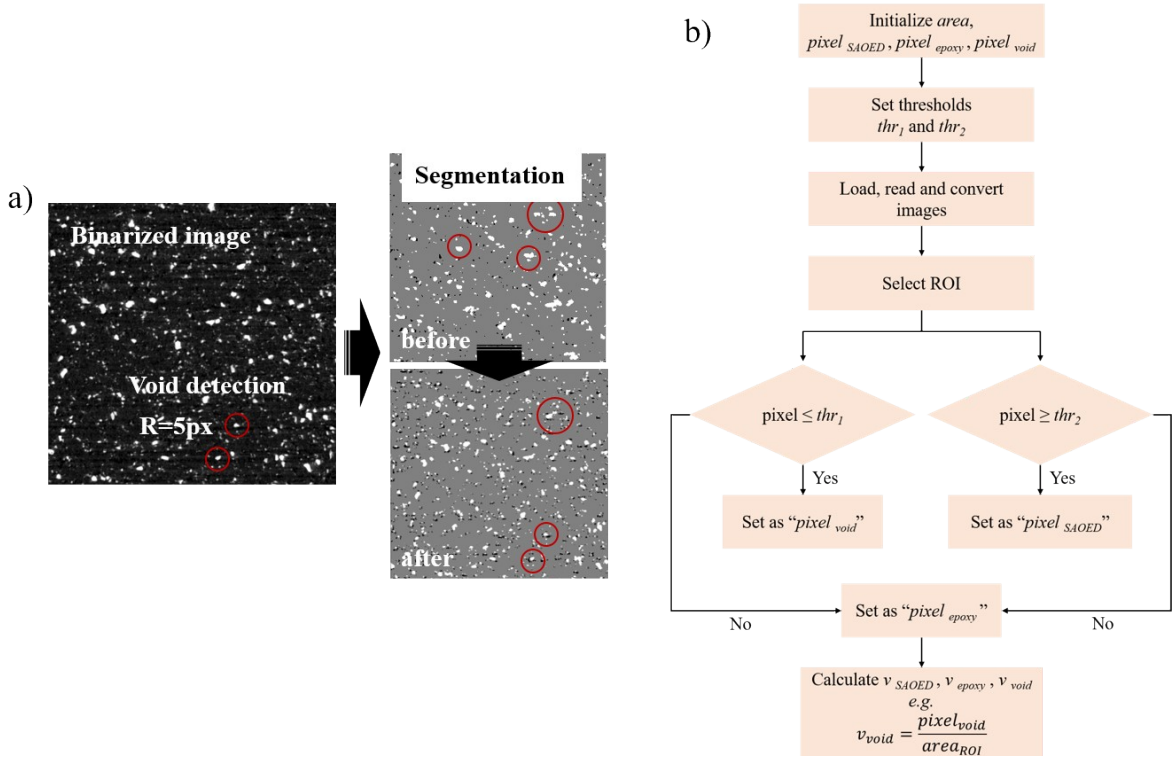

Figure S5: a) XRM images converted to binary images to perform segmentation b) Segmentation algorithm to distinguish void formation around SAOED particles

6. ML stress sensors after self-healing

In self-healing epoxy vitrimer systems, ensuring that any enhancement after thermal treatment is related to self-healing bond exchange reactions rather than post-curing is crucial. For this, the curing state of ML stress sensors should be explored directly after their synthesis and after the self-healing procedure. FTIR peak analysis is performed by comparing the area under the epoxide ring in DGEBA resin ($A_{epoxide}^{before}$) and cured ML stress sensors ($A_{epoxide}^{after}$) according to Eq.1:

$$Degree\ of\ curing = \left(1 - \left(\frac{A_{epoxide}^{after}}{A_{epoxide}^{before}}\right)\right) x100 \qquad \text{Eq.1}$$

Table S4 shows that 20-ML/VT and 20-ML/SVT are cured at around 99% and 95%, respectively. After self-healing, the curing degree of 20-ML/SVT becomes 96.5% with a slight increment. Since there is no significant change in the curing state of 20-ML/SVT after self-healing, Figure S6 verifies that the ML recovery is primarily related to self-healing bond exchange reactions.

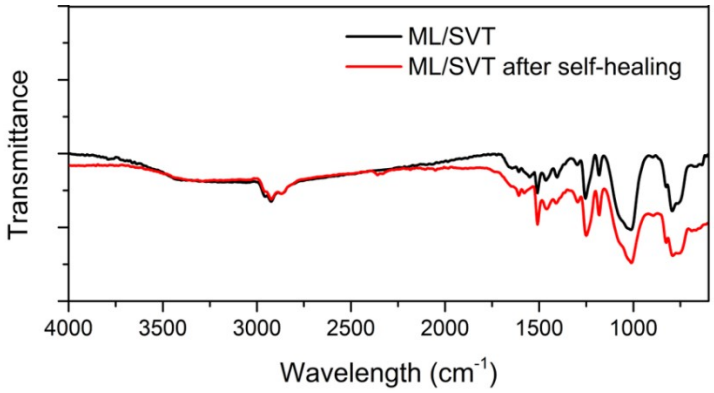

Figure S6: FTIR analysis of as-produced and self-healed 20-ML/SVT

Table S4: FTIR peak analysis results demonstrating the curing degree in ML stress sensors

Sample	$A_{epoxide}^{before}$	$A_{epoxide}^{after}$	$Degree\ of\ curing$ (%)
DGEBA	622.25	-	-
ML/VT	-	5.85	99.1%
ML/SVT	-	30.92	95.0%
ML/SVT after self-healing	-	21.67	96.5%

7. References

1. Wu, X.; Yang, X.; Yu, R.; Zhao, X.-J.; Zhang, Y.; Huang, W., A facile access to stiff epoxy vitrimers with excellent mechanical properties via siloxane equilibration. *Journal of Materials Chemistry A* **2018,** *6* (22), 10184-10188.